Epitaxial growth, structure, and composition of Fe films on GaAs(001)-2×4

E. Kneedler, P. M. Thibado, B. T. Jonker,[a] B. R. Bennett, B. V. Shanabrook, R. J. Wagner, and L. J. Whitman
Naval Research Laboratory, Washington, DC 20375-5343

(Received 27 November 1995; accepted 1 April 1996)

The structure and composition of Fe films grown on As-terminated GaAs(001)-2×4 surfaces at 175 °C has been studied *in situ* with scanning tunneling microscopy (STM), photoelectron diffraction (PED), and x-ray photoelectron spectroscopy (XPS). The GaAs surfaces were prepared by molecular beam epitaxy (MBE) and exhibited large atomically well-ordered terraces. We find that the 2×4 reconstruction has a significant impact on the Fe nucleation and growth, with initial nucleation occurring at As-dimer sites. STM reveals that the first half-monolayer of Fe forms small two-dimensional islands along the As-dimer rows before growing onto the adjacent Ga-rich rows, with no evidence of substrate disruption. PED indicates that the growth is predominantly layer by layer, with the growth front for the nth deposited layer limited to the $(n+1)$th layer. XPS spectra show that the Fe films include a concentration gradient of Ga and As out-diffused from the interface, with some of the As segregating to the Fe surface, similar to previous results obtained for growth on non-MBE prepared GaAs surfaces. Possible mechanisms for the film growth and the origins of the intermixing are discussed.

I. INTRODUCTION

The behavior of magnetic thin films on semiconductor substrates is of great practical interest due to the potential for integrating such films into novel semiconductor heterostructure devices. For very thin films, the magnetic and electronic properties of the heterostructure may depend strongly on the nature of the metal/semiconductor interface. This dependence can arise from the atomic-scale structure of the interface, the occurrence of interdiffusion, or the nature of the initial film growth. Before magnetic heterostructure devices can be widely realized, the characteristics of the metal/semiconductor interface must be well understood.

One magnetic system of special interest is Fe on GaAs, which is considered to have one of the most well-ordered and abrupt metal/semiconductor interfaces. Fe grows epitaxially (bcc) on GaAs (110) and (001), with the film crystallographic axes coincident with those of the substrate, due in part to the fact that the bcc Fe lattice constant is approximately half that of zinc-blende GaAs ($2a_{\mathrm{Fe}}/a_{\mathrm{GaAs}}=1.013$).[1,2] Although the films are epitaxial, studies of Fe deposition on both cleaved GaAs(110) and sputter-annealed (001)-$c(8\times2)$ surfaces have found the growth to be three-dimensional (3D) and observed Ga and As intermixed in the first ~50 Å of Fe.[3,4] Magnetic measurements of Fe films on GaAs(001) revealed anomalous behavior, with films as thick as 200 Å exhibiting substantially lower magnetization than expected from bulk properties.[5] Furthermore, such films often have an in-plane uniaxial component to the magnetic anisotropy,[5] although an ideal bcc Fe(001) film should have fourfold symmetry.

One factor that may contribute to the magnetic anisotropy is the substrate surface reconstruction, which is thought to influence the Fe nucleation and growth[6]; no studies have yet focused on this effect, however. A more complete understanding of the magnetic behavior requires a detailed description of both the physical and compositional structure of the Fe films. In this article we describe the structure and composition of Fe films grown on the As-terminated GaAs(001)-2×4 surface, which is the most commonly utilized surface for the growth of compound semiconductor device structures. The samples were prepared by molecular beam epitaxy (MBE) and characterized *in situ* with scanning tunneling microscopy (STM), photoelectron diffraction (PED), and x-ray photoelectron spectroscopy (XPS). We find that the 2×4 surface reconstruction has a significant impact on the Fe nucleation and film growth, with initial nucleation occurring at As-dimer sites.

II. EXPERIMENT

The experiments were performed in a multichamber ultrahigh vacuum (UHV) molecular beam epitaxy and surface analysis facility consisting of two MBE chambers, a PED/XPS chamber, and an STM chamber, all connected via a UHV sample transfer system. The GaAs(001) surface was prepared via homoepitaxial MBE growth on a silicon-doped substrate oriented within 0.1° of (001). After growing a 1-μm-thick buffer layer of Si-doped GaAs ($n\sim10^{17}/\mathrm{cm}^3$) at 580 °C, a 300 Å layer of undoped GaAs was grown at a reduced rate combined with growth interrupts to eliminate Si contamination of the surface and produce large well-ordered terraces. The substrate was then cooled to 550 °C under an As flux from a valved cracker source, at which point the As source was both valved and shuttered. The sample was cooled further to 200 °C under no flux prior to transfer to another chamber. This procedure consistently produced an atomically well-ordered, As-dimer terminated (2×4)-reconstructed surface as indicated by reflection high energy electron diffraction (RHEED) and confirmed by STM.[7]

Fe deposition was performed primarily in a second MBE chamber using a high-temperature Knudsen cell source at a

[a]Electronic mail: jonker@anvil.nrl.navy.mil

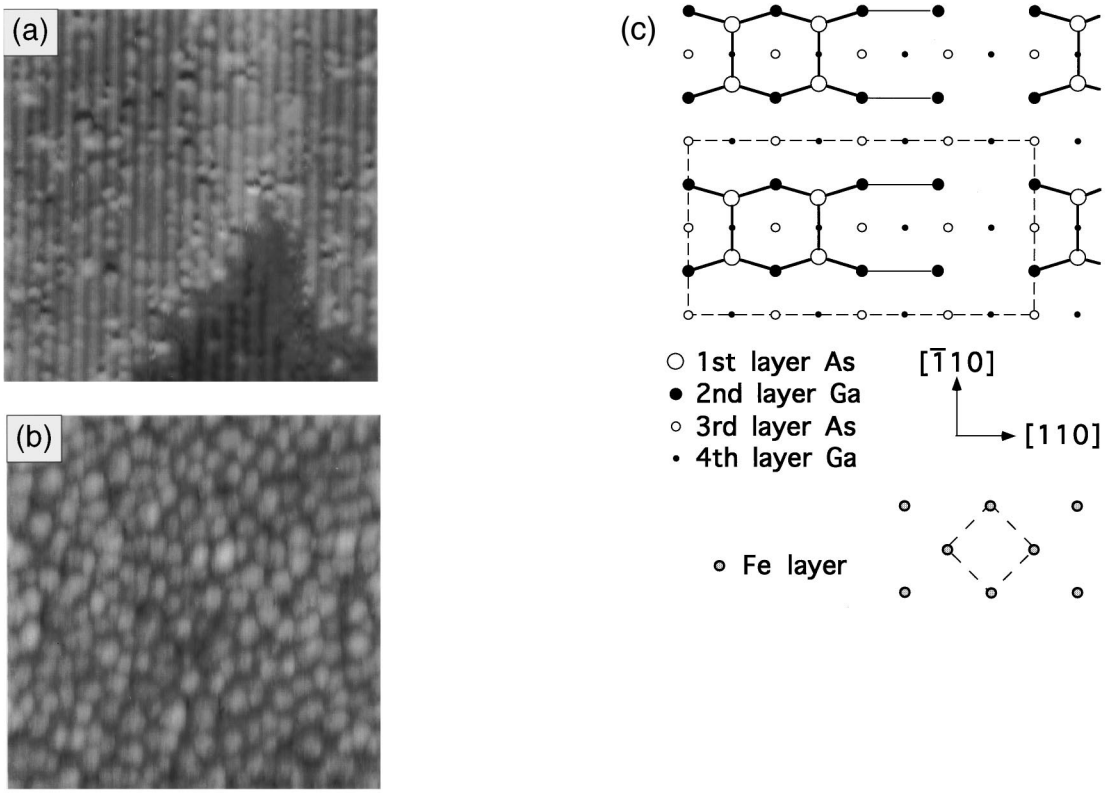

FIG. 1. (a) Filled state STM image (3 V) of 0.1 ML Fe on GaAs(001)-2×4. Image size 380 Å×380 Å. A v-shaped step edge, 2.8 Å high, is visible in the lower part of the image. (b) Filled state image (3 V) of 0.5 ML Fe. The surface corrugation is 1–2 Å. (c) Model of the 2×4 reconstructed surface, and the bcc (001) surface.

rate of 0.05 monolayer/s. We define 1 monolayer (ML)$\equiv 1.22\times10^{15}$ atoms/cm^2, corresponding to the atomic density of the bcc Fe(001) plane, which is approximately twice the atomic density of the bulk terminated GaAs(001) surface (and would produce a film ~1.4 Å thick if deposited uniformly). For the XPS core level measurements, the evaporations were performed in the PED/XPS chamber at a rate of 0.025 ML/s with an electron-beam heated rod evaporator.[8] The substrate temperature was 175 °C for all Fe depositions. The Fe deposition sources were regularly calibrated by x-ray fluorescence measurements performed on thick films (~50 Å). Relative Fe coverages were also confirmed by XPS.

After Fe growth the sample was cooled to room temperature and transferred to one of the other chambers for study. All data were collected with the sample at or slightly above room temperature. PED and XPS spectra were recorded using a monochromatized Al $K\alpha$ source and a 120 mm hemispherical analyzer with an angular resolution of ±3° (PED) and ±15° (XPS). Sample motion was computer-controlled via a stepper motor-driven two-axis goniometer, with the angle between the x-ray source and analyzer fixed at 70.8°. High resolution core level spectra ($\Delta E = 0.6$ eV) were recorded at an emission angle of 15° from the surface to maximize surface sensitivity. STM images were acquired with a constant current of 0.1 nA and a sample bias of −3.0 V and are displayed in gray scale.

III. RESULTS AND DISCUSSION

A filled-state STM image of a surface covered with 0.1 ML of Fe, the lowest coverage examined, is displayed in Fig. 1(a). At this coverage most of the surface is unperturbed GaAs(001)-2×4, with bright rows oriented along the [1$\bar{1}$0] direction (spaced 16 Å apart) and a small corrugation visible along each row (every 8 Å). As illustrated in Fig. 1(c), the structure of this surface is believed to consist of rows of As-dimer pairs separated by Ga-terminated rows (where the As-dimer pairs are missing[9]); the bright rows observed in the STM image are associated with the rows of As dimers. The deposited Fe gives rise to the bright ''bumps'' that occur almost exclusively on the As-dimer rows, typically covering one dimer pair. The association of these features with Fe (and not surface defects, for instance) was confirmed by multibias imaging: whereas the Fe-related features become much more prominent at lower bias voltages, the appearance of typical defects observed on an Fe-free surface has little bias dependence.[7] These results indicate that the Fe adatoms preferentially adsorb on the As-dimer rows, forming 2D islands with an average diameter of 8 Å. It is important to note that the 2×4 surface reconstruction remains intact on the sites adjacent to the Fe islands, demonstrating that any disruption of this surface is limited to atomic-scale reactions between the Fe and As dimers in the immediate 2×4 unit cell.

The STM image obtained after 0.5 ML of Fe deposition is shown in Fig. 1(b). Although the surface is almost completely covered by 2D Fe islands, the rowlike structure of the (2×4) substrate reconstruction is still evident in the general alignment of the islands: the islands are elongated along the $[\bar{1}10]$ direction with an average size of 15 Å by 25 Å as determined from the 2D autocorrelation function. The islands are now typically wider than the As-dimer rows, indicating that Fe adsorption, initially confined to the dimer rows, has now taken place on the missing dimer (Ga-terminated) rows. The fact that the islands appear flat suggests that they are at least two Fe layers thick in these Ga-terminated areas. Although most Fe islands are approximately the same height, a small fraction of them appear noticeably higher, consistent with some additional Fe growth on the predominantly flat islands.

Whereas STM provides an excellent view of the atomic-scale surface topography following Fe deposition, PED and XPS provide complementary information regarding the structure and composition within the Fe overlayers. The integrated Fe 2*p* emission intensity as a function of polar emission angle for a range of Fe coverages between 0.5 and 31 ML is shown in Fig. 2. At this kinetic energy (772 eV) the photoelectrons are in the forward scattering regime, so that intensity maxima are expected along the directions of near-neighbor atoms (i.e., along low-index directions) [Fig. 2(c)]. In particular, the low-index directions within bulklike crystals produce well-defined peaks. Each peak in the PED spectrum for the 31-ML-thick Fe film, for example, can be identified with a low-index direction within a bcc crystal, as labeled in Fig. 2.

Since forward scattering can be observed only when atoms are above the plane of the emitting atom, the information provided by PED can be utilized to determine early growth morphology.[10] If the angle-dependent emission of an adsorbate is measured for a series of coverages, the onset of forward-scattering peaks at angles which characterize the structure signals the occupation of second, third, or fourth layer sites. A single atomically flat monolayer, for example, would produce no forward-scattering peaks, while 2 ML of layer-by-layer bcc growth would result in a single peak in the [111] direction (for the [110] azimuth). If the absolute growth rate is known, multilayer growth or clustering can be identified during deposition of the first few monolayers by the occurrence of forward-scattering peaks corresponding to the occupation of $(n+1)$th layer sites well before completion of the nth monolayer.

The polar scan along the [110] azimuth for 0.5 ML of Fe on GaAs(001)-2×4 clearly shows a maximum in the [111] direction [Fig. 2(a)], indicating that some second layer sites are already occupied. Although the PED spectra do not reveal the identity of the second layer scatterers (e.g., Fe versus As), spectra along the [110] and $[1\bar{1}0]$ azimuths are equivalent, demonstrating that the occupied sites have a bcc-like structure. (Note that this would not be the case if the emitting Fe atoms were substitutionally embedded in the zinc-blende substrate.) These data indicate that the Fe adatoms are bonding either above or within the surface plane of the As dimers, with minimal disruption of the substrate surface, concurrent with some occupation of second Fe monolayer sites before completion of the first layer. These results are consistent with the STM results, which indicated that some bilayer Fe growth may occur both between the As-dimer rows and on top of the initial 2D islands. Note that within the resolution of the PED spectra, no evidence for third layer occupation is yet observed.

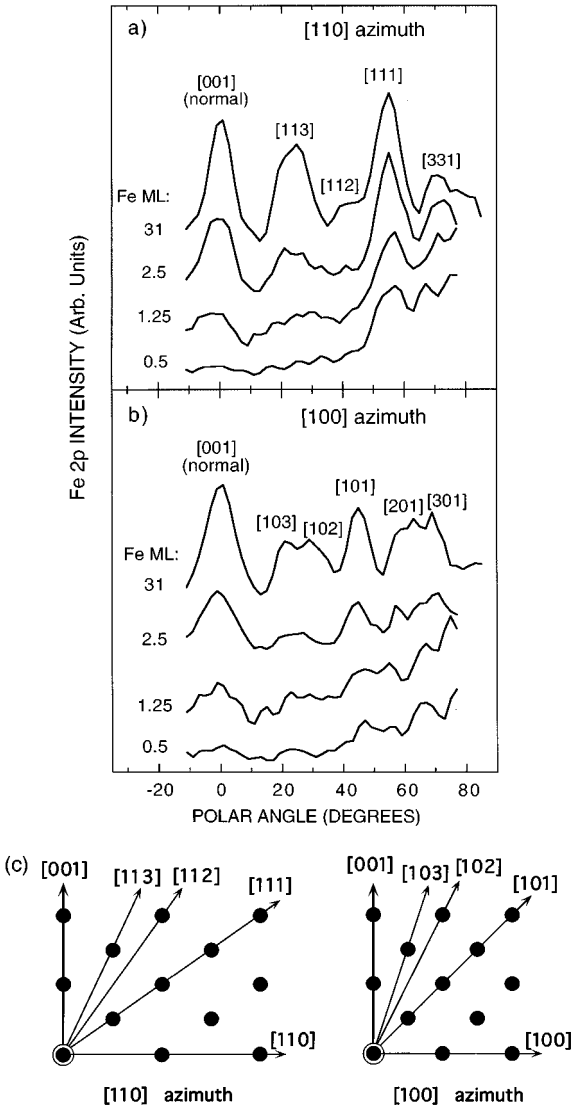

FIG. 2. (a) Fe 2*p* photoelectron polar diffraction spectra in the [110] azimuth (electron kinetic energy=772 eV) as a function of Fe coverage on GaAs(001)-2×4. The spectra are vertically offset for clarity. (b) Spectra in the [100] azimuth. (c) An illustration of forward-scattering conditions in the [110] and [100] projections for a multilayer bcc (001) film. Note that the observation of specific forward-scattering peaks can be correlated with occupation of particular layer sites within the film.

The PED data obtained at a coverage of 1.25 ML exhibit a strong peak along [111] for scans in the [110] azimuth, and weaker peaks along [101] in the [100] azimuth and along [001] for polar scans in both azimuths (Fig. 2). The [111] peak signals the expected occupation of second layer sites,

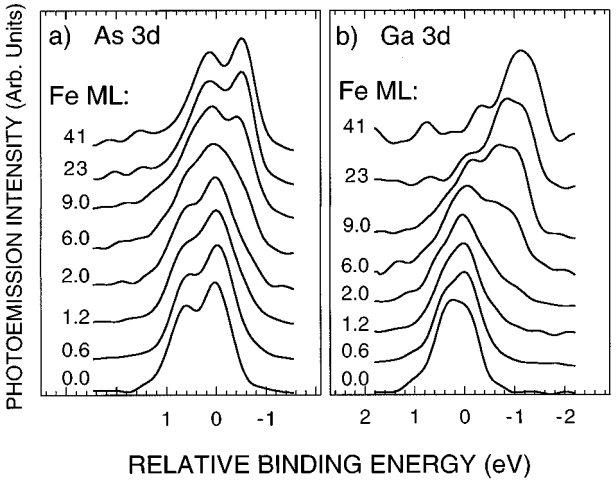

FIG. 3. XPS spectra of As and Ga 3*d* core levels as a function of Fe coverage on GaAs(001)-2×4. Each spectrum has been normalized to its peak intensity and vertically offset for clarity. Core levels shown for clean GaAs have been shifted 0.15 eV to lower binding energy to compensate for band bending.

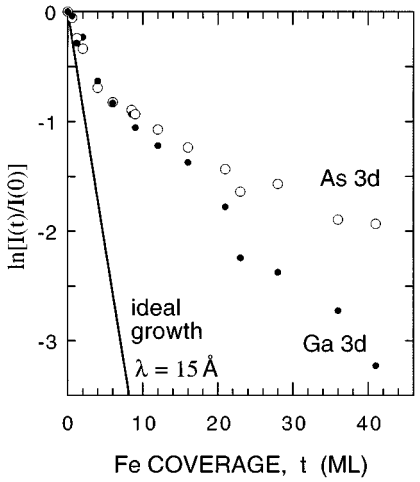

FIG. 4. Normalized Ga and As 3*d* core level intensities as a function of Fe coverage. The attenuation of the substrate levels expected for ideal Fe layer-by-layer growth (without interdiffusion) is shown for comparison as the solid line, calculated for an emission angle of 15° from the surface and an electron mean free path of 15 Å.

whereas the appearance of the [101] peak suggests occupation of some third layer bcc-like sites. Although the weak [001] peak is also indicative of third layer occupation in a simple forward-scattering picture, single-scattering calculations[11] show that this peak has contributions from higher order diffraction effects associated with the first two layers. Since this [001] peak appears together with the [101] peak, we interpret it here as further evidence for slight third layer site occupation.

As the third equivalent monolayer of Fe is deposited, the PED polar scans begin to exhibit most of the features typical of bulklike films, as can be seen by comparing the 2.5 and 31 ML data of Fig. 2. For 2.5 ML, peaks along [001] and [101] are pronounced due to the formation of the third layer, as expected, and some fourth layer site occupation is indicated by the appearance of a peak in the [113] direction. However, the absence of peaks in the [112] and [102] directions implies that there is no significant fifth layer site occupation during growth of the third ML. We thus observe that Fe grows in a predominantly layer-by-layer fashion, with the growth front for the nth deposited layer limited to the $(n+1)$th layer. Although sites in the $(n+1)$th layer are occupied before the nth layer is completed, extreme 3D growth such as that observed on the Fe/GaAs(110) system[12] can be ruled out for Fe/GaAs(100)-2×4 from our PED and STM results. For coverages $\leqslant$3 ML, the PED and STM data generally show the formation of predominantly flat islands with some multilayer growth occurring, but little or no tendency towards 3D clustering or significant disruption of the substrate.

The elemental composition of the Fe films is elucidated by XPS measurements as a function of Fe coverage. As shown in Figs. 3 and 4, both Ga and As can be detected even for the higher coverages studied (41 ML). Since the STM data show the GaAs surface to be completely covered by a uniform Fe overlayer after the first few monolayers[7] and the mean free path for the As and Ga 3*d* photoelectrons is ~15 Å, we attribute the persistance of these signals to out-diffusion of Ga and As from the interface. The nature of these out-diffused atoms is revealed somewhat by the 3*d* core level spectra, which evolve considerably with increasing Fe coverage (Fig. 3). Two regimes are evident: (i) coverages less than ~2 ML, where the levels show little change; and (ii) higher coverages, where distinctly shifted core levels appear. In the first regime, which we associate with the bonding of Fe to the GaAs surface, the As level broadens slightly with little change in binding energy, and the Ga level shows a slight shift in spectral weight towards lower binding energy. If this behavior is interpreted simply in terms of charge transfer accompanying bonding with the Fe adatoms, it reflects an increase in charge density on the Ga atoms but little change on the As. These features are consistent with interfacial bonding between Fe and As and concomitant debonding between As and Ga. For coverages of a few monolayers, the core levels give no indication of Fe-induced substrate surface disruption, consistent with the STM and PED results.

As the Fe coverage is increased (>2 ML), a second regime of behavior is observed in which the substratelike Ga and As 3*d* features are replaced by peaks at lower binding energy that show a considerable evolution in character with coverage. Within the resolution of our experiment, at least one new peak is observed for both the As and Ga levels, as seen in the spectra for a 6-ML-thick film. While the new As 3*d* feature is relatively constant in binding energy as a function of coverage, the Ga 3*d* spectra exhibit a more complex coverage dependence, with the new peak(s) shifting continuously to lower binding energy. For a 41-ML-thick Fe film, the net shift is 0.45 eV for the new As 3*d* doublet and 1.15 eV for the Ga, and the peaks associated with bulk GaAs are no longer observed. (The signal-to-noise ratio of the spectra

is poor at higher coverages, and the small-amplitude oscillations at higher binding energy are residues of the smoothing and background subtraction and are not considered significant.) The abrupt change in character of the 3*d* levels suggests that both Ga and As atoms are being displaced from the interface after the formation of a few monolayers of Fe, i.e., after the Fe film has assumed a metallic character. Similar core level shifts observed for Fe on GaAs(110) have been associated with Ga and As atoms multiply coordinated with Fe atoms in an increasingly metallic environment.[3]

The persistence of As and Ga 3*d* signals for thicker Fe films is illustrated in Fig. 4. The reduced intensity, defined as $\ln[I(t)/I(0)]$ where t is the Fe film thickness, is plotted for the As 3*d* and Ga 3*d* levels as a function of Fe coverage. The behavior expected for layer-by-layer growth without interdiffusion is included for comparison as the solid line. At coverages up to 2 ML, the experimental data are in reasonable agreement with this ideal growth. At coverages above 2 ML, however, the data depart significantly from this ideal behavior due to As and Ga out-diffusion. Although the Ga intensity continues to decrease monotonically, it does so much more slowly than expected. The As signal also initially decreases, but then plateaus at ~10% of its initial intensity, suggestive of As surface segregation. This behavior is qualitatively similar to that observed previously[3,4] and demonstrates that while Ga out-diffusion and incorporation is limited to the interface region, some As continuously segregates to the Fe surface.

The exact location of the out-diffused As atoms is expected to play an important role in understanding the modified magnetic behavior of the Fe film. Chambers *et al.* proposed an interstitial face-centered As site within the Fe film based on an anomalous feature in electron-stimulated Fe *LMM* Auger electron diffraction spectra from bcc Fe films grown on a sputter-annealed GaAs(001)-$c(8\times2)$ surface.[13] To determine the sites of the out-diffused As in our samples, we have performed polar scans of the intensity of the photon-stimulated As $L_3M_{45}M_{45}$ Auger level (kinetic energy of 1225 eV) as shown in Fig. 5. It is important to consider contributions to the emission from substrate As atoms, which is significant at near-normal angles. For polar angles >45°, however, we believe that substrate contributions become small relative to near-surface As emission. The features in both azimuths at large polar angles suggest significant As occupation of subsurface bcc sites [see Fig. 2(c)]. The overall increase in intensity at larger polar angles suggests that some of the As is also adsorbed on the surface of the Fe film, as observed for growth on the $c(8\times2)$ surface. We observe no indication for an fcc interstitial As site.

The observed out-diffusion of Ga and As at higher coverages must be reconciled with the fact that the STM images show no evidence of surface disruption during the initial nucleation of the Fe overlayer. Although the STM images provide little insight regarding the composition of the quasi-ordered 2D islands observed along the As-dimer rows, one would expect any exchange reactions with the surface atoms to result in a more disordered surface topography than is

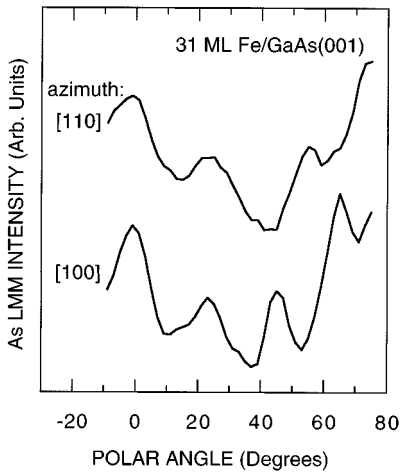

FIG. 5. Photoelectron diffraction spectra of the photon-stimulated As $L_3M_{45}M_{45}$ Auger transition (kinetic energy=1225 eV) for the [110] and [100] azimuths. Note that the spectra have many of the features characteristic of a bcc structure [see Fig. 2(c)].

observed. In addition, the core level data indicate that significant disruption of the substrate surface occurs only after deposition of 2–3 ML of Fe. A possible scenerio which accounts for the origin of the out-diffused Ga and As and the corresponding driving mechanism is proposed as follows: we speculate that the Fe would ideally like to bond to an As-terminated bulklike (1×1) surface. One pathway to such a surface on GaAs(001)-2×4 is for the Fe to initially bond to the As-dimer rows and then, with increasing coverage, to bond to less favorable Ga atoms between the dimer rows (in the second GaAs layer). As the film grows, Fe at some point (~2 ML) displaces the Ga atoms in this substrate layer, including those below the As-dimer rows. This results in an Fe/As interface and frees one layer of Ga and a half layer of As (from the dimer rows) for out-diffusion into the growing Fe film. Given that the onset of out-diffusion appears to be correlated with the onset of metallicity, we further speculate that the displacement of the second layer (substrate) Ga atoms and first layer As is driven by the accompanying change in chemical potential at the interface. The liberated Ga and As atoms are incorporated within the growing film, while a fraction of the As segregates to the surface.

IV. CONCLUSIONS

We have studied the nucleation and growth of Fe on MBE-grown GaAs(001)-2×4 at 175 °C using *in situ* STM, PED, and XPS. STM reveals that Fe initially forms small 2D islands along the As-dimer rows before growing onto the adjacent Ga-rich rows; the images show no evidence of substrate disruption. PED shows that the Fe grows in a predominantly layer-by-layer mode, with the growth front for the nth deposited layer limited to the $(n+1)$th layer. As previously observed for Fe grown on GaAs(001)-$c(8\times2)$ and GaAs(110), the films include a gradient of Ga and As con-

centrations, with some of the As segregating to the Fe surface. We speculate that As in the (2×4) dimer rows and the second substrate layer Ga are displaced by the Fe in order to make an Fe/As interface, and that this disruption is driven by a chemical potential gradient created when the Fe film becomes metallic with increasing thickness.

ACKNOWLEDGMENTS

This work was supported by the Office of Naval Research. Two of the authors (E. K. and P. M. T.) further acknowledge support by National Research Council Postdoctoral Fellowships at the Naval Research Laboratory.

[1]G. A. Prinz and J. J. Krebs, Appl. Phys. Lett. **39**, 397 (1981).
[2]J. R. Waldrop and R. W. Grant, Appl. Phys. Lett. **34**, 630 (1979).
[3]M. W. Ruckman, J. J. Joyce, and J. H. Weaver, Phys. Rev. B **33**, 7029 (1986).
[4]S. A. Chambers, F. Xu, H. W. Chen, I. M. Vitomirov, S. B. Anderson, and J. H. Weaver, Phys. Rev. B **34**, 6605 (1986).
[5]J. J. Krebs, B. T. Jonker, and G. A. Prinz, J. Appl. Phys. **61**, 2596 (1987).
[6]B. T. Jonker, *Epitaxial Growth Processes*, Proc. SPIE **2140**, 118 (1994).
[7]P. M. Thibado, E. Kneedler, B. T. Jonker, B. R. Bennett, B. V. Shanabrook, and L. J. Whitman, Phys. Rev. B R10481 (1996).
[8]B. T. Jonker, J. Vac. Sci. Technol. A **8**, 3883 (1990).
[9]J. Zhou, Q. Xue, H. Chaya, T. Hashizume, and T. Sakurai, Appl. Phys. Lett. **64**, 583 (1993).
[10]S. A. Chambers, Adv. Phys. **40**, 357 (1991).
[11]D. J. Friedman and C. S. Fadley, J. Electron Spectrosc. Relat. Phenom. **51**, 689 (1990).
[12]R. A. Dragoset, P. N. First, Joseph A. Stroscio, D. T. Pierce, and R. J. Celotta, Mater. Res. Soc. Symp. Proc. **151**, 193 (1989).
[13]S. A. Chambers, I. M. Vitomirov, S. B. Anderson, H. W. Chen, T. J. Wagener, and J. H. Weaver, Superlattices Microstructures **3**, 563 (1987).